SINTEF
PROCEEDINGS
2

Proceedings of the 12th International Conference on Computational Fluid Dynamics in the Oil & Gas, Metallurgical and Process Industries

Progress in Applied CFD – CFD2017

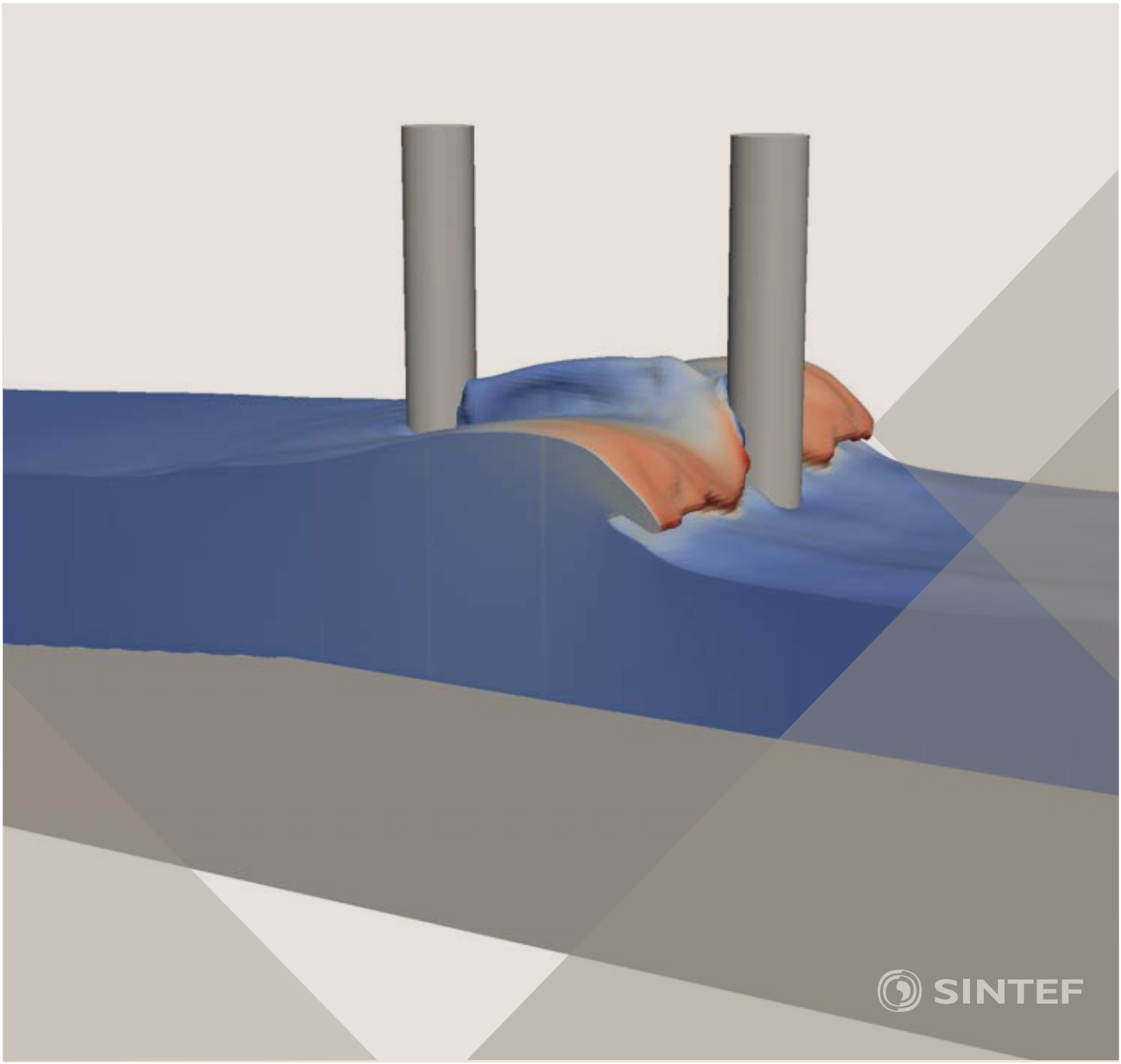

SINTEF Proceedings

Editors:
Jan Erik Olsen and Stein Tore Johansen

Progress in Applied CFD – CFD2017

Proceedings of the 12th International Conference on Computational Fluid Dynamics in the Oil & Gas, Metallurgical and Process Industries

SINTEF Academic Press

SINTEF Proceedings no 2
Editors: Jan Erik Olsen and Stein Tore Johansen
Progress in Applied CFD – CFD2017
Selected papers from 10th International Conference on Computational Fluid Dynamics in the Oil & Gas, Metallurgical and Process Industries

Key words:
CFD, Flow, Modelling

Cover, illustration: Arun Kamath

ISSN 2387-4295 (online)
ISBN 978-82-536-1544-8 (pdf)

SINTEF Academic Press
Address: Forskningsveien 3 B
PO Box 124 Blindern
N-0314 OSLO
Tel: +47 73 59 30 00
Fax: +47 22 96 55 08

www.sintef.no/byggforsk
www.sintefbok.no

SINTEF Proceedings
SINTEF Proceedings is a serial publication for peer-reviewed conference proceedings on a variety of scientific topics.
The processes of peer-reviewing of papers published in SINTEF Proceedings are administered by the conference organizers and proceedings editors. Detailed procedures will vary according to custom and practice in each scientific community.

PREFACE

This book contains all manuscripts approved by the reviewers and the organizing committee of the 12th International Conference on Computational Fluid Dynamics in the Oil & Gas, Metallurgical and Process Industries. The conference was hosted by SINTEF in Trondheim in May/June 2017 and is also known as CFD2017 for short. The conference series was initiated by CSIRO and Phil Schwarz in 1997. So far the conference has been alternating between CSIRO in Melbourne and SINTEF in Trondheim. The conferences focuses on the application of CFD in the oil and gas industries, metal production, mineral processing, power generation, chemicals and other process industries. In addition pragmatic modelling concepts and bio-mechanical applications have become an important part of the conference. The papers in this book demonstrate the current progress in applied CFD.

The conference papers undergo a review process involving two experts. Only papers accepted by the reviewers are included in the proceedings. 108 contributions were presented at the conference together with six keynote presentations. A majority of these contributions are presented by their manuscript in this collection (a few were granted to present without an accompanying manuscript).

The organizing committee would like to thank everyone who has helped with review of manuscripts, all those who helped to promote the conference and all authors who have submitted scientific contributions. We are also grateful for the support from the conference sponsors: ANSYS, SFI Metal Production and NanoSim.

Stein Tore Johansen & Jan Erik Olsen

Organizing committee:

Conference chairman: Prof. Stein Tore Johansen
Conference coordinator: Dr. Jan Erik Olsen
Dr. Bernhard Müller
Dr.Sigrid Karstad Dahl
Dr.Shahriar Amini
Dr.Ernst Meese
Dr.Josip Zoric
Dr.Jannike Solsvik
Dr.Peter Witt

Scientific committee:

Stein Tore Johansen, SINTEF/NTNU
Bernhard Müller, NTNU
Phil Schwarz, CSIRO
Akio Tomiyama, Kobe University
Hans Kuipers, Eindhoven University of Technology
Jinghai Li, Chinese Academy of Science
Markus Braun, Ansys
Simon Lo, CD-adapco
Patrick Segers, Universiteit Gent
Jiyuan Tu, RMIT
Jos Derksen, University of Aberdeen
Dmitry Eskin, Schlumberger-Doll Research
Pär Jönsson, KTH
Stefan Pirker, Johannes Kepler University
Josip Zoric, SINTEF

CONTENTS

UNRESOLVED CFD-DEM IN ENVIRONMENTAL ENGINEERING: SUBMARINE SLOPE STABILITY AND OTHER APPLICATIONS

Alice HAGER[1*] , Manuela KANITZ[2], Jürgen GRABE[2], Christoph KLOSS[1], Christoph GONIVA[1]

[1] DCS Computing GmbH, 4020 Linz, AUSTRIA

[2] TUHH, Institute of Geotechnical Engineering and Construction Management, 21079 Hamburg, GERMANY

* E-mail: alice.hager@dcs-computing.com

ABSTRACT

When installing gravity foundations for offshore structures such as wind power stations or oil platforms, the seabed needs to be excavated for providing enough stability. To minimize the impact on the surrounding fauna and the installation costs, steep but stable slopes are desired. The work presented is done in a research project on the numerical investigation of the stability of submarine slopes, particularly under the impact of influences like material removal or wave-induced disturbances.

The method used in the current project is coupled CFD-DEM: while the dynamics of the fluid phase (water and in some cases water and air) are handled with computational fluid dynamics (CFD), the soil is modelled by spheres, whose motion is calculated with a discrete element method (DEM). Force models are used for considering the particles' effect on the fluid and vice versa, a void fraction field accounts for the volume of the particles on the CFD side. Due to the high number of particles in the domain only unresolved CFD-DEM (cf., e.g. Zhou (2010)) is suitable: in this case the particles are smaller than the cells of the CFD mesh.

In the presented work the investigations concentrated on the validation of the CFD-DEM models against small-scale experiments that were conducted by the authors. In a first step, the used materials were characterized and a lubrication force model was implemented. Furthermore, some basic investigations on the topic of dilatancy were carried out. Then an experimental setup and an according simulation were compared. In addition to that a three phase (air, water, particles) solver was used to depict the effect of surface waves onto the particle bed.

For the calculations CFDEM®coupling was used. CFDEM®coupling is an Open Source software for coupled CFD-DEM simulations. It uses the CFD framework of the Open Source CFD code OpenFOAM® and the DEM framework of the Open Source code LIGGGHTS®. Both CFDEM®coupling and LIGGGHTS® have been presented before (cf., e.g. Goniva et al. (2012), Kloss et al. (2012)), the used model equations were validated against analytical solutions and literature.

Keywords: Lagrangian methods, granular flows, unresolved CFD-DEM.

NOMENCLATURE

Greek Symbols

α Volume fraction.
ρ Mass density, [kg/m^3].
μ Dynamic viscosity, [kg/m.s].
ω Angular velocity, [rad/s].

Latin Symbols

F Force, [N].
g Gravitational acceleration, [m/s^2].
h Minimal surface distance of two particles, [m].
m Mass, [kg].
p Pressure, [Pa].
r Particle radius, [m].
U Velocity, [m/s].
v Velocity [m/s].
R_{sl} Solid-liquid interaction force, [kg/(m.s)^2].
T Torque, [N.m].

Sub/superscripts

f Fluid
i Index i
j Index j
p Particle
w Wall

INTRODUCTION

The reasons for producing under water slopes are manifold: they occur when sand or gravel is harvested as well as when foundations for off-shore wind power plants or oil platforms are required. For both economic and ecological reasons it is desirable to build steep and yet stable slopes. The stability of the slopes and their formation can either be influenced by the production process itself (e.g. grab or suction dredging) or environmental phenomena such as surface waves. A joint research project between TUHH and DCS Computing GmbH aims on modelling different phenomena at the soil-water interface. The presented contents were developed within the course of this project.

First, the implementation and validation of a lubrication force model is discussed and the capability of depicting

dilatancy is demonstrated. Modelling the effect of dilatancy is crucial for simulating saturated sand beds. Due to shear loading, dilatancy leads to a local hardening of the soil bed as the pore volume increases. This effect causes a negative excess pore water pressure and hence suction occurs until the inflowing pore water fills the volume between the soil grains. In a second part two application cases are considered:

(i) the effect of suction dredging on an underwater slope is investigated numerically and compared to experimental data

(ii) a three-phase solver is used to proof the feasibility of simulating wave induced disturbances on particle beds

The presented work is realized with the Open Source software packages LIGGGHTS® (Kloss et al. (2012)) and CFDEM®coupling (Goniva et al. (2012)).

MODEL DESCRIPTION

A coupled CFD-DEM model was used to compute the dynamics of the fluid and particle phases and their interaction. On the CFD side the computational domain was discretised and a finite volume solver was applied. For the granular phase a Lagrangian method was used, in which each particle was considered individually.

Governing equations

The governing equations for the presented CFD-DEM method are the volume averaged Navier-Stokes equations:

Continuity equation

$$\frac{\partial \alpha_f \rho_f}{\partial t} + \nabla \cdot \left(\alpha_f \rho_f U\right) = 0 \qquad (1)$$

Momentum equation

$$\frac{\partial \alpha_f \rho_f U}{\partial t} + \nabla \cdot \left(\alpha_f \rho_f U U\right) = -\alpha_f \nabla p + R_{sl} + \alpha_f \rho_f g \qquad (2)$$

The term R_{sl} denotes the fluid-structure interaction force density, which is computed with the aid of particle-data. In the DEM method used for the calculation of the particle phase, the trajectory of each particle is calculated separately, using Newton's second law:

$$m_p \frac{dU_p}{dt} = \sum F_{p,p} + \sum F_{p,w} + m_p g + F_p + F_f \qquad (3)$$

$$I_p \frac{d\omega_p}{dt} = T_p \qquad (4)$$

The right-hand side of equation (3) consists of the particle-particle and particle-wall interaction forces, for their calculation a soft-sphere approach was used. The term $m_p g$ represents the mass-force due to gravity and F_p stands for the pressure forces. The term F_f represents the forces exerted by the fluid. In the current case the drag force, the pressure gradient force and the viscous force were identified as dominating forces. The drag force model by Koch and Hill (2001) was used. As the particle-particle contacts take place under water also a lubrication force model was implemented and validated.

Lubrication force model

If two particles collide within a fluid the displacement of the fluid in the gap between them causes a force – the lubrication force. While for many processes where fluids with relatively low viscosities are present the effect of the force is negligible, it might be worth considering in the presented applications. The classical formulation of the lubrication force is given as

$$F_{\text{lub}} = -6 \cdot \pi \cdot \mu \cdot r_{ij}^2 \cdot \left(\frac{1}{h}\right) \cdot v_n, \qquad (5)$$

where r_{ij} is the effective radius defined as

$$\frac{1}{r_{ij}} = \frac{1}{r_i} + \frac{1}{r_j}, \qquad (6)$$

with i and j denoting arbitrary different particles. h is the minimal surface distance between two particles and one has to make sure that the lubrication force does not become infinitely large when the particles are in contact with each other. Therefore, the radius of action of the lubrication force was limited to a certain minimal distance between two particles. This approach was also used by Sun and Xiao (2016) in their implementation.

Validation of the lubrication force model

In the considered cases particle-particle interactions have by far more impact than particle-wall interactions. Therefore, also the validation test-case focused on particle-particle interaction: a sphere was fixed at a specific position while another sphere was released "directly" above it, with different initial velocities and for different fluid viscosities.

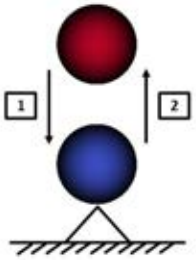

Figure 1: Basic test case for the validation of the lubrication force model.

During the simulation, the velocity of the moving particle was measured right before and after the collision. The velocity before the impact, v_1, was used to calculate the Stokes number as following (cf., e.g. Tomac (2013)):

$$St = \frac{m v_1}{6\pi\mu r^2}. \qquad (7)$$

The coefficient of restitution was determined as

$$c_{rest} = \frac{v_2}{v_1}. \qquad (8)$$

In the diagram in Fig. 2 the coefficients of restitution for different fluid viscosities are displayed over the according Stokes numbers. The results of the implemented model are compared to values presented by Zhang et al. (2005) and by Tomac and Gutierrez (2013), a good accordance could be obtained.

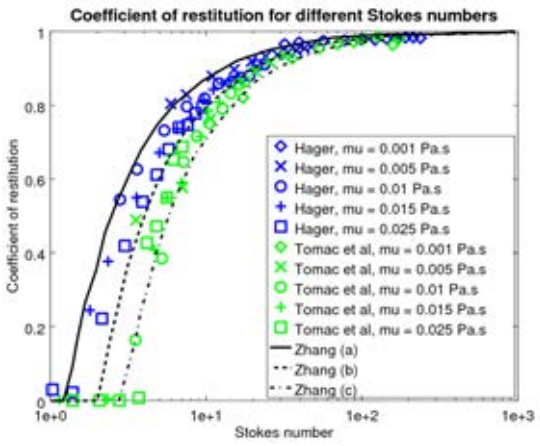

Figure 2: Validation of the lubrication force model.

Depiction of dilatancy

The qualitative test for demonstrating the capability of depicting dilatancy was the following: three packings with the same volume but of different volume fractions were generated (0.75, 0.80, 0.85), the packings consisted of about 3000 particles. For keeping the particle packing in place, fixed side walls were chosen, while the upper and the lower wall were moving: for the top wall a so-called servo wall was used that exerted a constant pressure force on the bed, while the lower wall was moved horizontally. The force of the servo wall was chosen such that the particle bed was at an equilibrium at the beginning of the test.

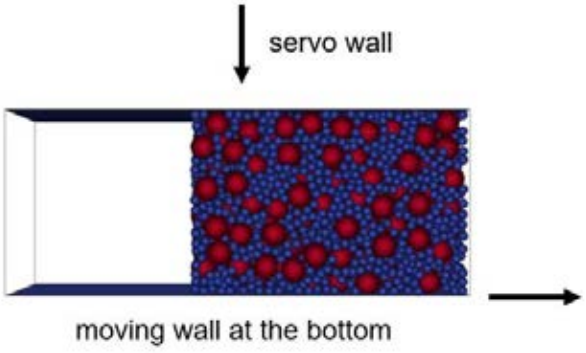

Figure 3: Setup of the dilatancy test case.

As soon as the motion of the lower wall started, the particles started to re-arrange and thus expand. The expansion showed in a lifting of the top plate, increasing with increasing initial volume fraction (cf. Fig. 4).

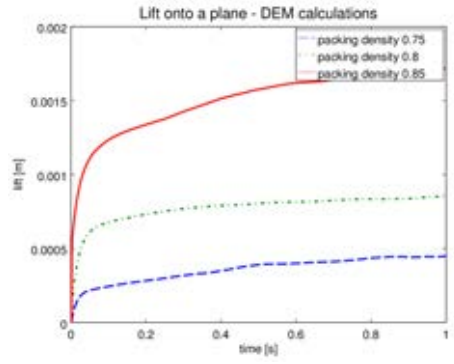

Figure 4: Displacement of the upper wall for different packing densities.

With this simple test the ability to depict dilatancy could be shown.

FORMATION OF UNDER WATER SLOPES

When extracting sand and gravel from under-water regions one often uses suction dredgers. In this process pumps deliver sand/gravel and water mixtures. Grabe (2005) presented a detailed small-scale experimental study of the effect of grab dredging onto the formation of an under-water slope. The material used in the experiments was described as sand with a critical angle of friction of 34°.

Material calibration

Accurate simulations require detailed knowledge of the used material. The material parameters can be divided in two groups: Some quantities can be measured directly, like for example density, grain size distribution or the volume fraction, while the set of model parameters needs to be determined otherwise. These describe the physical behaviour of the bulk material. Examples are the coefficient of friction and the coefficient of rolling friction. For obtaining these coefficients, a set of three well-established calibration experiments and simulations was conducted:

1. The shear cell test

The coefficient of friction between the particles can be determined with a shear cell. For the experiments Jenike shear testers with cylinder diameters of about 10 cm were used. These devices consist of an upper and a lower hollow cylinder which are filled with the granular material. One of these cylinders is fixed, the other one can be displaced linearly in horizontal direction. For the tests a weight is placed on top of the granular material (exerting a normal force) and the non-fixed cylinder is moved slowly in horizontal direction. The resulting shear stress is measured and compared to the shear stresses obtained by the ring shear cell test in the simulation.

Figure 5: Calibrating the particle-particle coefficient of friction with shear cell experiments and simulations.

2. Inclined plate

This experiment serves the purpose of determining the coefficient of rolling/sliding friction between particles and a wall. A small sample of grains is placed on a plate which is then inclined gradually. From a certain inclination (target angle) particles start to roll or slide down the plate, depending on whether the sliding or rolling friction is stronger.

Figure 6: Inclined plate test.

In the simulation particles are placed on a horizontal plate and the gravity vector is chosen such that the target angle is obtained. One then looks for the smallest coefficient of rolling friction, for which the particles are at rest (cf., Fig. 7).

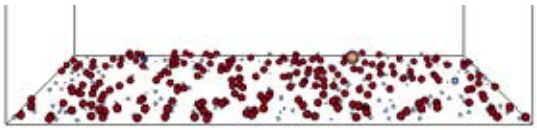

Figure 7: Simulation of the inclined plate test.

3. Angle of repose

The angle of repose experiment is used to determine the particle-particle coefficient of rolling friction. The setup used for the test is the following: a hollow cylinder is placed on an elevated circular plate with the same diameter as the cylinder. The cylinder is filled with granular material and the lifted slowly and uniformly, which leads to the formation of a conical heap. In the simulation the coefficient of rolling friction is varied until the angle of the cone matches the result of the experiment (cf., Fig. 8).

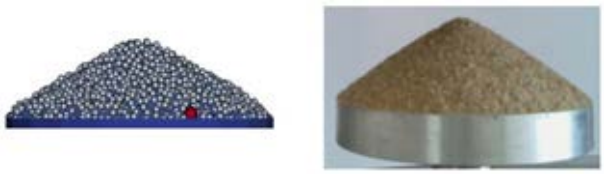

Figure 8: The particle-particle coefficient of rolling friction dominates the formation of the angle of repose.

The grain size distribution was identified by sieving, the average coefficient of restitution was determined with drop tests.

Simulation setup

As the experiment was carried out in a small scale it was possible to simulate the process at original scale. A slope with an inclination angle of 30° (smaller than the critical angle) was generated (cf., Fig. 9). The simulation domain had a length of 40 cm and a height of 25 cm. The maximal height of the particle bed was 20 cm. For reducing the number of particles in the simulation domain periodic boundary conditions were used for the front and back wall both on the CFD and the DEM side. The complete set of velocity and pressure boundary conditions is summed up in Table 1. The bed was initialized with a pure DEM calculation.

	velocity (U, m/s)	pressure (p, Pa)
top	zeroGradient	fixedValue (0)
bottom	fixedValue (0,0,0)	zeroGradient
front/back	cyclic	cyclic
left wall	fixedValue, (0,0,0)	zeroGradient
right wall	zeroGradient	fixedValue (0)

Table 1: Velocity and pressure boundary conditions for the CFD calculation.

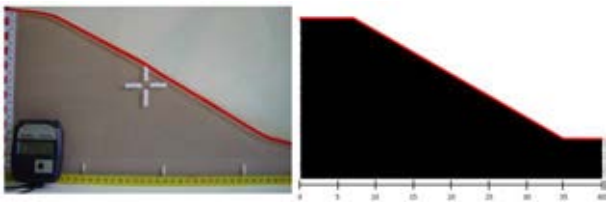

Figure 9: Initial slope (experiment vs. simulation)

In the current investigation, the focus lay on the formation of the slope after the extraction of the particles, thus the particles were removed at once in the simulation (cf., Fig. 10).

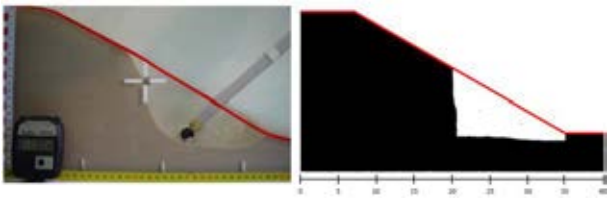

Figure 10: Slope after suction dredging is completed.

Results

After the removal of the particles in the dredging region the coupled CFD-DEM calculation was launched and the settling process started. In Fig. 11 two images of unstable slopes during the settling process in experiment and simulation are compared.

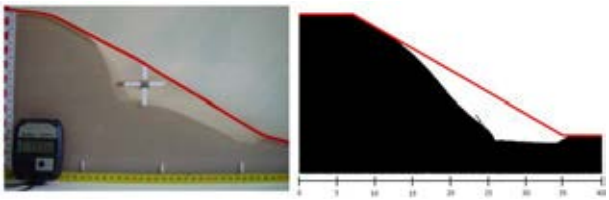

Figure 11: Slope during settling process (unstable).

It can be observed that while the reformation of the slope is ongoing, it develops slightly different in simulation and experiment. Furthermore, the time scale is smaller in the simulation, i.e. the changes of the slope occur faster. This difference could stem from an under-representation of the pore pressure in the simulation, but will be subject to future investigations as well. However, as can be seen in Fig. 12, in both cases the resulting final slope has an inclination of about 34°, which is the critical angle of the sand used.

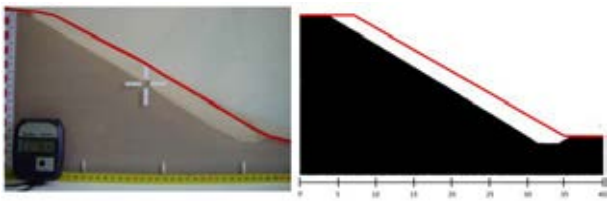

Figure 12: Final slope.

WAVE INDUCED DISTURBANCES

The purpose of this application example was to show the feasibility of combining a three-phase solver (two-phase fluid and particles) with the wave generation toolbox

waves2foam (cf., Jacobsen et al. (2011)). waves2foam uses a zone in which the waves are generated. For making sure that the manipulations of the equations due to wave generation and those due to the presence of a granular phase do not interfere, a separate wave generation zone without particles was used (cf., Fig. 13). The granular material used for these calculations were 3mm glass beads, their properties were determined as described in the previous section. The total length of the CFD domain was 1.2 m, whereas the first 0.4 m were used as wave generation zone. The height of the domain was 0.2 m and due to the application of periodic boundary conditions a domain depth of 0.05 m could be used.

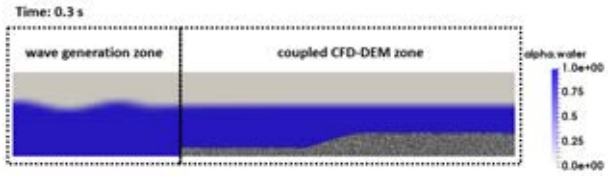

Figure 13: The waves were generated in a zone without particles.

As can be seen in Fig. 14 the waves propagate through the whole domain, their shape is influenced by the ascending sea bed.

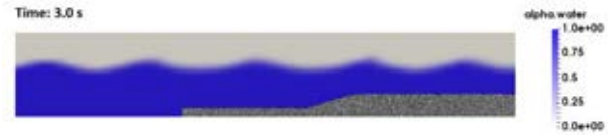

Figure 14: The waves propagate through the whole domain; the particle bed influences their shape.

When considering the force which the fluid exerts on the particle bed (here termed as drag force), the influence of the waves onto the soil becomes visible (cf. Fig. 15). The higher/lower force values onto the particles are in direct relation with the fluid pressure field ρ_{rgh} (total pressure minus hydrostatic pressure): it is lower underneath wave throughs and higher in wave crest areas and acts similar as a lift force.

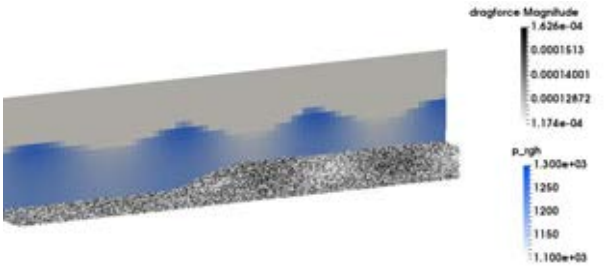

Figure 15: underneath the wave throughs the drag force onto the particles is increased while it is decreased underneath the wave crests.

These calculations showed that it is possible to apply wave boundary conditions to three phase problems within CFDEM®coupling. The observed behaviour matches the expectations and future experiments will be used for validation.

CONCLUSION AND OUTLOOK

A lubrication force model was implemented and validated and it was demonstrated that dilatancy can be depicted. The simulation of a suction dredging case was in good accordance with the experiments. Furthermore, the feasibility and plausibility of the combination of a three-phase solver and the toolbox waves2foam was shown by a small-scale test case, experiments for validating the new solver are planned.

ACKNOWLEDGEMENTS

The authors are grateful to the Austrian Science Fund (FWF) for supporting this research under project I 2257 (DACH project).

REFERENCES

GONIVA, C., KLOSS, C., KUIPERS, J.A.M. and PIRKER, S., (2012), "Influence of rolling friction modelling on single spout fluidized bed simulations", *Particuology*, **10** (5), 582-591.

GRABE, J., (2005), "Phänomene an der Grenzschicht zwischen Wasser und Boden", *Grenzschicht Wasser und Boden – Phänomene und Ansätze, Veröffentlichungen des Instituts für Geotechnik und Baubetrieb der TU Hamburg-Harburg*, **9**, 3-30.

JACOBSEN, N.G., FUHRMAN, D.R. and FREDSØE, J., (2011), "A wave generation toolbox for the open-source CFD library: OpenFOAM®", *Int. J. Numer. Meth. Fluids*, **70** (9), 1073-1088.

KLOSS, C., GONIVA, C., HAGER, A., AMBERGER, S. and PIRKER, S., (2012), "Models, algorithms and validation for opensource DEM and CFD-DEM", *Prog. Comput. Fluid. Dy.*, An. Int. J. 2012, **12** (2/3), 140-152.

KOCH, I. and HILL, R.J., (2001), "Inertial effects in suspension and porous-media flows", *Ann. Rev. of Fluid Mechanics*, **33**, 619-647.

OpenCFD Ltd., (2004-2017), "OpenFOAM – The Open Source CFD-toolbox", URL: www.openfoam.com.

SUN, R. and XIAO, H., (2016), "SediFOAM: A general-purpose, open-source CFD-DEM solver for particle-laden flow with emphasis on sediment transport", *Comput. Geosci.*, **89**, 207-219.

TAESERI, D., LAUE, J., OTSUBO, M. and TOWHATA, I., (2016), "New mitigation method for pipeline uplift during seismic event", *Geotechnical Research*, **3** (2), 54-64.

TOMAC, I. and GUTIERREZ, M., (2013), "Discrete element modelling of non-linear submerged particle collisions", *Granul. Matter*, **15**, 759-769.

ZHANG, W., NODA, R. and HORIO, M., (2005), "Evaluation of lubrication force on colliding particles for DEM simulation of fluidized beds", *Powder Technol.*, **158**, 92-101.

ZHOU, Z.Y., KUANG, S.B., CHU, K.W. and YU, A.B., (2010), "Discrete particle simulation of particle-fluid flow: model formulations and their applicability", *J. Fluid Mech.*, **661**, 482-510.